The Thesis committee for Alfredo Raul Hijar Santibanez

Certifies that this is the approved version of the following thesis:

Evaluating river cross section geometry for a hydraulic river routing model: Guadalupe and San Antonio River Basins

APPROVED BY
SUPERVISING COMMITTEE:

Supervisor:_____

Ben R. Hodges

_____

David Maidment

Evaluating river cross section geometry for a hydraulic river routing model: Guadalupe and San Antonio River Basins

by

Alfredo Raul Hijar Santibanez, B.S.E.

Thesis

Presented to the Faculty of the Graduate School
of the University of Texas at Austin
in Partial Fulfillment
of the Requirements
for the Degree of

Master of Science in Engineering

The University of Texas at Austin
May, 2015

Acknowledgements

I would like to express my very great appreciation to some individuals and institutions for their valuable help and constructive suggestions during this work. First, I would like to offer my special thanks to my research advisor, Dr. Ben R. Hodges, for his very patient guidance and his enthusiastic encouragement. My grateful thanks are also extended to the invaluable assistance of Dr. Frank Liu, as well as the EWRE faculty Professor, Dr. David Maidment, and the help provided by the PhD students, Gonzalo Espinosa and Fernando Salas, at the University of Texas at Austin. Finally, I wish to acknowledge the help provided by all the EWRE faculty and stafff of the University of Texas at Austin.

This material is based upon work supported by the National Science Foundation under Grant No. CCF-1331610.

Evaluating river cross section geometry for an hydraulic river routing model: Guadalupe and San Antonio River Basins

by

Alfredo Raul Hijar Santibanez, MSE

The University of Texas at Austin, 2015

SUPERVISOR: Ben R. Hodges

A new methodology is presented to construct reliable river channel cross section approximations. These approximations are based on the idea of downstream hydraulic geometry as well as supported by the information collected by the USGS streamflow measurement stations across the study area. A hydraulic river routing model (SPRNT) is run with the newly constructed cross section approximations. Initial conditions for the simulation are estimated based on the steady state solution for the model. Boundary conditions or lateral inflows for the river network are estimated based on the outputs of a Land Surface model: Noah, which provides surface and sub-surface runoff for every catchment area in the San Antonio and Guadalupe river basins. Simulations are compared with observed measurements from the USGS stations.

Table of Contents

List of Figures

List of Tables

Chapter 1 - Introduction

1.1 Motivation

Flow routing techniques are a key component to understand and forecast environmental impacts as well as hydrological processes, such as reservoir operations, floods, aquatic habitat assessments, among others. Flow routing may be classified as either lumped or distributed. Lumped or hydrological flow routing schemes compute flow as a function of time at one location along the watercourse. Distributed or hydraulic flow routing schemes compute flow as a function of time and space along the watercourse (Maidment, 1993).

Data requirements are substantially different for both models. From a practical point of view, lumped models, which require less information, are more attractive and are widely used in academia and industry. Distributed models are based on physical laws (i.e. mass and momentum conservation) and require more detailed information describing river or channel geometry, friction, and lateral fluxes. The later models are more suitable for determining floodplain depths, real-time forecasting of river floods, inundation maps for dam-break events, and estimating backwater effects due to downstream constrictions (Hicks, 1996; Maidment, 1993; Pramanik et al., 2010).

Channel cross section geometry has a controlling influence on the shape of flood waves, velocity and sediment transport capacity in the channel as well as in the floodplain through overbank and subsurface pathways (Western and Finlayson, 1997;

Chang, 1988; Richards, 1982). Regional variation in river cross section geometry has been a main concern for hydrologists for flow routing (Snell and Sivapalan, 1995).

Despite the advancement in computational speed and the proliferation of distributed models over the last two decades, many agencies and researchers continue to study and use hydrological models for large-scale river network flow routing. As stated by (Hicks, 1996), this is because large-scale flow routing problems involve hundreds of kilometers long reaches or river networks at a regional or continental scale, and the cost of obtaining the necessary information (i.e. channel cross section geometry and its resistance characteristics) over such large distances is considered to be economically and physically unfeasible. Moreover, availability of measured river cross sections is scarce for most regions around the globe.

Given that channel or river cross section geometry is a prime input for hydraulic models, there is a key importance in obtaining that information. Simple cross-sectional hydraulic geometry relations were introduced by Leopold and Maddock (1953) to describe the hydraulics of river cross sections and variation in channel dimensions throughout river networks. They described empirical relations between channel top width (w), channel mean depth (d) and channel mean velocity (v) and channel discharge (Q).

Recent studies by Pramanik et al. (2010); Gichamo et al. (2012) took advantage of the development of satellite-gathered information as well as from digital eleva-

tion models (DEM) to extract river cross section geometries and simulate river flow routing. This means that there is an on-going research which focuses on developing software tools to extract spatial features that would be useful for hydraulic models from topographical sources (Tesfa et al., 2011; Merwade et al., 2008). Other studies try to use data assimilation techniques to identify a synthetic river cross-section that is hydraulically equivalent to the real river geometry (Honnorat et al., 2006; Roux and Dartus, 2008).

Furthermore, effective catchment-scale management of flooding, floodplains, sediment and nutrient transport, and river habitats requires the evaluation of river cross section geometry throughout river networks (Stewardson, 2005). Hence, the key open question on data requirements remains: What is the level of cross-sectional detail that is actually needed for hydraulic models, vice the data detail that is typically obtained in surveys?

The motivation for this research was the development of data sets combining surveyed and estimated channel geometry over large river basins. Ideas from hydraulic geometry combined with historical stage-discharge data are used to develop reliable cross-sectional data, which is useful where surveyed data are unavailable. Although it is likely that for the foreseeable future we will not have comprehensive survey data for entire river basins, we can significantly advance our science if we use the data we have to estimate geometry for solution with the full dynamic equations rather than *a-priori* reducing the physical processes represented.

1.2 Research Objectives

The objectives of this research are to: (1) develop a novel methodology to approximate river cross section geometry for river networks where there is scarcity of river channel data, (2) link a Land Surface Hydrology model with a flow routing scheme, considering the lagging of the catchment runoff into the streams, to describe the flood wave of every reach within a particular river basin, (3) create the *netlist*, a syntax for river network topology using a set of defined blocks, for our study area, and (4) run the Simulation Program for River Networks (SPRNT) for the Guadalupe and San Antonio rivers basins and compare its results with measurements in selected stations from the United States Geological Survey (USGS). The initial difference between the SPRNT simulations and the USGS streamflow stations measured data is used to calibrate the hydraulic routing model (Manning's n).

When the hydraulic routing model is calibrated and the simulated results are in close agreement with the observed stations, we will have a better understanding of the capabilities and limitation of SPRNT as an hydraulic routing model.

1.3 Research Overview

This research presents a novel and reliable method to approximate river cross section geometry based on available USGS streamflow measurement stations. More-

over, the SPRNT model is linked with the Community Noah Land Surface Model, which provides lateral inflows for the river network. Finally, SPRNT is run for the Guadalupe and San Antonio river basins.

The river network topology is described in the netlist (Hodges, 2013; Liu, 2012). The netlist incorporates the river cross section geometry, providing the relationships between the channel depth and cross sectional area, as well as cross sectional area and channel roughness, with sufficient robustness and reliability to be used in one-dimensional dynamic models. This work examines the performance range of a cross-section approximation as well as relationships readily known data (e.g. slopes, mean annual flow rate) and geometry that can be used where cross-sectional data is unavailable. Results of the model are compared with measured data at USGS streamflow measurement stations in the river network to determine the accuracy of the calibration and uncertainty of the model.

Chapter 2 - Background

2.1 Hydraulic Geometry

Some hydraulic characteristics can be described by the hydraulic geometry formulation introduced by Leopold and Maddock (1953). Throughout the last 60 years, the scientific community has been studying hydraulic geometry and its relationships in different river environments worldwide. Results of these studies demonstrate that the utility of hydraulic geometry is unquestioned (Gleason, 2015) as well as the application of hydraulic geometry for hydraulic routing models. However, the underlying physical principles that produce hydraulic geometry behavior have yet to be satisfactorily uncovered.

This study introduces a novel methodology for approximating river cross sections. The following literature review presents the origin of hydraulic geometry, as well as studies that support the application of hydraulic geometry. In the present work, a statistical approach is used to determine the relationship between the channel hydraulic characteristics along the Guadalupe and San Antonio River Basins, instead of the power law formulation from hydraulic geometry. The channel cross section approximations are used in the Simulation Program for River Networks (SPRNT), a fully dynamic Saint-Venant equation solver (Hodges, 2013).

Leopold and Maddock (1953) related channel cross section shape parameters with channel discharge as simple power function. There are two different approaches

regarding the hydraulic geometry relations: *at-a-site* hydraulic geometry, and *downstream* hydraulic geometry. *At-a-site* hydraulic geometry relates the hydraulic variables at any given cross section, while *downstream* hydraulic geometry links together the hydraulic variables downstream along a stream network under the condition that discharge at all points is equal in frequency of occurrence. The hydraulic geometry relationships aim to describe and predict changes in the hydraulic variables and are expressed as follows:

$$w = aQ^b \tag{1}$$

$$d = cQ^f \tag{2}$$

$$v = kQ^m \tag{3}$$

$$L = pQ^j \tag{4}$$

where w is the stream top width, d is the stream mean depth, v is the stream mean velocity, L is the suspended-sediment load, and Q is the water discharge. a, c, k, p are numerical coefficients, while b, f, m, j are numerical exponents [1]. The hydraulic variables (e.g. w, d, Q, v and L) play a key role in determining channel cross section shape and the changes in its shape downstream (Leopold and Maddock, 1953). The functions derived for *at-a-site* and *downstream* hydraulic geometry differ in the numerical values of the coefficients.

[1]These coefficients and exponents are empirical parameters that are used to fit specific cases to approximate observed behavior

Application of hydraulic geometry relationships are varied as stated by previous researchers (Ferguson, 1986; Leopold and Maddock, 1953; Singh et al., 2003). Hydraulic geometry concepts have been used for streamflow monitoring activities, estimation of minimum requirements for fish or recreational purposes, assessment of fish habitat, design of irrigation channels, flow regulation schemes, among others. Hydraulic geometry relationships and coefficients can be similar for different river basins (Leopold and Maddock, 1953; Singh et al., 2003; Ferguson, 1986). In the downstream approach, the hydraulic variables (i.e. v, d, and w) increase with discharge, shaping the form of the channel cross section (Singh et al., 2003). Additionally, downstream hydraulic geometry may use an arbitrary discharge as reference. As an example, mean annual discharge or bank-full flow may be used for downstream hydraulic geometry in a particular river system (Leopold and Maddock, 1953; Singh et al., 2003).

Many authors have pursued empirical verification of hydraulic geometry for different rivers (Stall and Fok, 1968; Leopold and Miller, 1956; Ackers, 1964; Park, 1977; Rhodes, 1977). Richards (1976) noted that hydraulic geometry exponents can be employed to discriminate between different types of river sections, such as riffles or pools, up to bank-full stage. In terms of the power law validation, Chong (1970) stated that the hydraulic geometry relations were similar over varying environments. Regarding the stability of the hydraulic geometry relations, Parker (1979) has stated that the scale factors a, c, and k, vary from locality to locality but the exponents b, f, and m, exhibit a remarkable degree of consistency, and seem independent of location and only weakly dependent on channel type and material.

Part of the scientific community challenged the precepts of hydraulic geometry. Richards (1973) criticize the lack of solid theoretical justification for Leopold and Maddock (1953)'s work. He stated that there is no *a priori* reason why power functions should necessarily represent the relationship between the dependent variables and the discharge. Following this study, Park (1977); Rhodes (1977, 1987) compiled the results of previous hydraulic geometry investigations from Ackers (1964); Miller (1958); Brush (1961) and introduced the ternary *b-f-m* diagram. This diagram presents the $b - f - m$ numerical exponents of *at-a-site* hydraulic geometry. Figure 1 shows an example of a ternary diagram applied to hydraulic geometry.

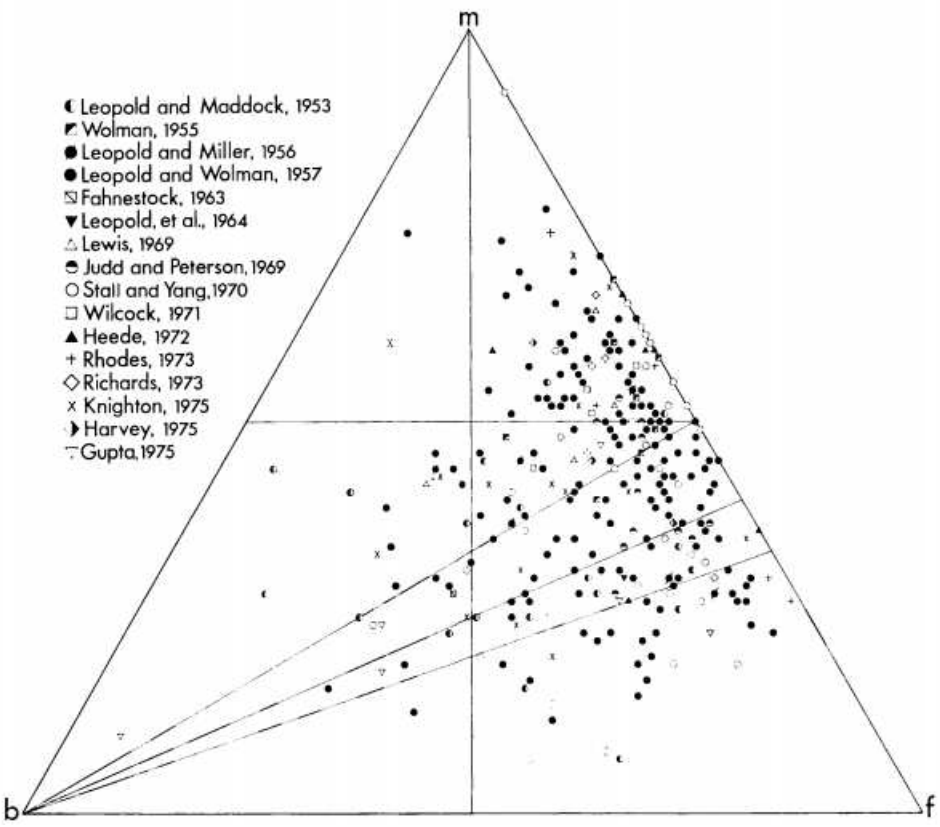

Figure 1: The b-f-m diagram showing plotting position of 315 set of at-a-station hydraulic geometry exponents (Rhodes, 1977).

Rhodes (1977, 1987); Park (1977) concluded that the exponents presented lit-

tle similarity across rivers and environments. At the time, the conclusion of Park (1977); Rhodes (1987) were a major departure as well as a challenge to Leopold and Maddock (1953) work.

Ferguson (1986) presented a key paper, which derived at-a-site hydraulic geometry for different channel geometries through the use of widely accepted empirical flow resistance equations (i.e. Manning and Darcy-Weisbach). Manning equation is presented herein:

$$V = \frac{1}{n} R^{2/3} S^{1/2} \tag{5}$$

where n is Manning roughness factor, R is hydraulic radius, and S is the slope of the hydraulic grade line. According to Ferguson (1986), from Manning equation velocity can be describe as a function of depth at a cross section. Then, the velocity can be estimated from Keulegan flow law (Gleason, 2015; Richards, 1976):

$$\frac{V}{\sqrt{gRS}} = 6 + 5.75 \log \frac{R}{k_s} \tag{6}$$

where k_s is the Nikuradse's equivalent roughness height. Velocity values and velocity-depth functions were set on different channel cross sections, which resulted in width as a function of depth. These relationships allowed Ferguson (1986) to recreate field data that would normally be collected to estimate at-a-site hydraulic geometry variables (Gleason, 2015). Ferguson (1986) concluded that *at-a-station* exponents are a function of cross sectional channel shape, and that the power law form of hydraulic

geometry is merely coincidental. Thus, according to Ferguson (1986), there should be no reason why the variables in hydraulic geometry should take the form of a power law.

Following Ferguson (1986), several theories regarding hydraulic geometry have been developed, each leading to unique relations between the channel shape parameters and channel discharge. (Rhoads, 1991; Phillips and Harlin, 1984) stated that the exponents and coefficients of hydraulic geometry relations of equations 2.1 vary from location to location on the same river and from river to river, as well as from the high flow range to the low flow range. Buhman et al. (2002) used a stochastic approach to study large spatial trends in *at-a-station* hydraulic geometry. Turowski et al. (2008) concluded that hydraulic geometry is particularly stable and well defined for bedrock channels.

In more recent studies, Mejia and Reed (2011) evaluate the effects of parameterized cross sections by developing a modeling framework and testing three cross section scenarios. Mejia and Reed (2011) recognize the importance and key role that cross sections play in a distributed context. Orlandini and Rosso (1998); Koren et al. (2004); Valiani and Caleffi (2009) have parameterized cross sections, in which a simple shape is assumed. Orlandini and Rosso (1998) showed that parameterized cross sections with vertically varying widths based on relationships of hydraulic geometry, as opposed to rectangular shapes with constant width, can lead to considerable improvement in flow simulations using a distributed model. Mejia and Reed (2011)

concluded that the scenario, where different power laws for the channel and floodplain portion were considered, showed improvements compared to other scenarios (less complex) and were comparable to the ones obtained from using detailed cross sections data.

2.2 Hydraulic River Channel Flow Routing

Large-scale river modeling presents several challenges for the scientific community (Hodges, 2013). One of this challenge arises from the need to model channels using accurate physics based flow equations to capture flow dynamics. This need implies a fully dynamic hydraulic routing model, which describes unsteady flow in a watercourse as a function of time and space. This model is based on the complete differential equation of one-dimensional unsteady flow (the Saint-Venant equations) (Hodges, 2013; de Saint-Venant, 1871). The original Saint-Venant equations are the *mass conservation equation*, i.e.,

$$\frac{\partial Q}{\partial x} + \frac{\partial A}{\partial t} = q_l \tag{7}$$

and the *momentum equation*, i.e.,

$$\frac{\partial Q}{\partial t} + \frac{\partial}{\partial x}\left(\frac{Q^2}{A}\right) + gA\frac{\partial h}{\partial x} = gA(S_o - S_f) \tag{8}$$

where the nonlinear friction slope is described by the Chezy-Manning equation:

$$S_f = n^2 \frac{Q^2}{A^2} \frac{1}{R^{4/3}} \tag{9}$$

One limitation of the fully dynamic Saint-Venant equations is the requirement of detailed river channel information. In choosing a hydraulic routing model for large-scale river networks, there is a classical trade-off between simplicity and precision. For this reason, several researchers and studies use simple routing conceptualization (Mejia and Reed, 2011) or reduced-physics models to simulate river flow dynamics (Paiva et al., 2011). However, there is concern that a simpler routing conceptualization may cause substantial loss of predictive capability (Cook and Merwade, 2009; Moreda et al., 2009; Horritt and Bates, 2002). Additionally, data availability should not be used as a reason to a priori reduce the modelled physics: the dynamic equations can be readily applied with either approximated or calibrated geometry when channel data is lacking (Hodges, 2013).

Fully dynamic hydraulic models are useful for determining floodplain depths, required heights of structures such as bridges or levees, and streamflow velocities (Maidment, 1993). These models can be also used to estimate sediment transport, which turns into a fundamental role for physical and biological studies. Recently, and with the help of new collection techniques and methodologies, entire river basins have been fully parameterized both using manually collected data and remote sensing products.

Different modelers have addressed the data requirement challenge for hydraulic routing in different ways, but to date there is no accepted best answer for this problem. Hicks (1996) evaluated the reliability of a hydraulic flood routing model based on limited cross section information for the case of the Peace River in British Columbia and Alberta. The hydraulic routing model was based on the fully dynamic Saint-Venant equations and assumed a rectangular channel cross section. Hicks (1996) concluded that a reliable hydraulic flood routing model can be developed with limited field data supplemented with topographic map data and cross section geometric assumptions.

A couple of years later, Orlandini and Rosso (1998) showed that parameterized cross sections with vertically varying widths based on relationships of hydraulic geometry, as opposed to rectangular shapes with constant width, can lead to considerable improvement in flow simulations using a diffusive wave routing model.

Based on the previous studies, Trigg et al. (2009) developed an hydraulic model to characterize the Amazon flood wave in the main channel. Full irregular cross sections perpendicular to the river center-lines were extracted from the interpolated bathymetry grid. Additionally, equivalent flow area, rectangular cross sections were derived from the irregular cross sections. The models used were the new LISFLOOD-FP diffusive channel solver and the HEC-RAS full hydrodynamic 1D Saint Venant model. Several tests were run to assess the effect of using a diffusive wave approxi-

mation as well as simpler channel geometries. Trigg et al. (2009) concluded that it is necessary to include at least the diffusion term in the hydraulic model for the studied reaches of the Central Amazon. Simpler cross section approximations yielded an error of 0.100.15 m in water level. Ignoring the full dynamic Saint-Venant equations introduced a further error in water elevation of the order of 0.020.03 m. Trigg et al. (2009) mentioned that these errors are very small in comparison to the mean annual flood wave amplitude of 1112 m. As seen by Trigg et al. (2009) study, it can be acceptable to use simpler cross section approximations for river with mean annual flood wave amplitude.

Similar to Trigg et al. (2009), Paiva et al. (2011) presented a full one-dimensional hydrodynamic model to calculate flow propagation on a complex river network. The model used the full dynamic SaintVenant equations and extracted channel parameters, such as river width, river depth, river cross section bottom level, and floodplain geometry, from relatively limited geographical data (i.e. SRTM DEM). Paiva et al. (2011) applied the hydrodynamic model on the Purus River basin, Brazil. The hydrodynamic model was capable of reproducing the main hydrological features of the Purus River basin, as well as realistic floodplain inundation maps.

Both studies (Paiva et al., 2011; Trigg et al., 2009) produced acceptable results given the hydrological setting. Nevertheless, the uncertainty of the models was not addressed by the researchers. In a more recent study, Sanyal et al. (2013) studied the adaptations and adjustments that are fundamental to use hydrodynamic models

like LISFLOOD-FP to describe flood waves by using freely available Shuttle Radar Topographic Mission digital elevation model (SRTM-DEM), available topographical maps and sparse network of river gauging stations. Sanyal et al. (2013) quantified the uncertainty in model outputs in a generalized likelihood uncertainty estimation framework to demonstrate the level of confidence that one can have on such flood routing approaches.

2.3 River Cross Section Extracion

Software tools have been, and still are, being developed to extract spatial features that are useful for hydraulic models from topographical data sources, both in GIS (Merwade et al., 2008) and non-GIS environments (Schwanghart and Kuhn, 2010; Gichamo et al., 2012). However, obtaining detailed topographical data for every river basin is still a challenging task due to economic and accessibility reasons (Gichamo et al., 2012; Pramanik et al., 2010).

A hydraulic model requires a sufficient representation of the river channel and floodplain geometries, with an accurate description of the model parameters, to make it possible to predict the water level and flood wave along the modeled reach or network accurately. The flow chart in Figure 2.3 outlines the steps followed by Gichamo et al. (2012) to construct the river cross-sections based on ASTER GDEM data and synthetic cross-sections by utilizing optimization.

Pramanik et al. (2010) proposed a novel methodology for extracting river cross-

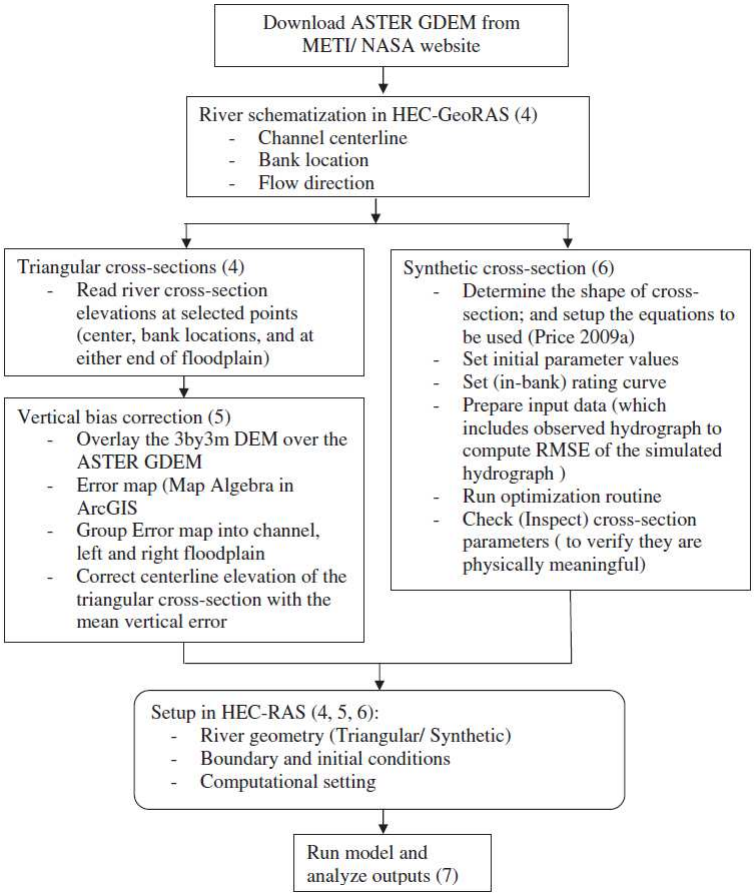

Figure 2: River cross section extraction methodology (Gichamo et al., 2012).

sections from SRTM-DEM of 3-arc second. The extracted river cross sections were used in the MIKE 11 hydrodynamic model to simulate the magnitude of the flood wave in the reaches of Brahmani river basin. The observed and simulated model results showed a close agreement.

Based on Pramanik et al. (2010)'s work, Gichamo et al. (2012) presented two approaches for the extraction of river cross-sections from a freely available, satellite-based Digital Elevation Model (DEM). The first method assumed a triangular cross section approximation defined by 5 points: stream centerline, bank stations, and boundary of the floodplains. The information for the triangular cross sections was extracted from elevation readings from the ASTER GDEM. The second approach used optimization methods to find the synthetic/standard cross section shapes. Through the used of data assimilation techniques, the synthetic cross sections were progressively refining themselves and were able to preserve sufficient description of channel hydraulic characteristics (Roux and Dartus, 2004). Gichamo et al. (2012) used the extracted cross sections (both triangular and synthetic) in a 1D river routing model (HEC-RAS) to simulate the flood wave of a part of the Tisza River in Hungary. The results indicated that both approaches for cross section extraction (triangular and synthetic) presented acceptable deviations from the hydrographs Gichamo et al. (2012) concluded that, even though the approaches have limitations, the methodology produces acceptable results and encourages to used the methodology in areas where topographic are is scarce.

In recent years, a new remote sensing technology, lidar, has been proved as a high resolution and accurate method for obtaining topographical data (Tsubaki and Kawahara, 2013; Mason et al., 2007). However, there are some limitations which affect the accuracy of such measurements (Podhoranyi and Fedorcak, 2015). Limitations include the following: (i) the topographic infrared LiDAR system is unable to penetrate water bodies as the laser beam is fully absorbed by the water, (ii) there are some situations when the laser beam is unable to reach the ground surface (Tsubaki and Kawahara, 2013), (iii) elevations cannot be measured directly in areas covered by vegetation or bridges, and (iv) accurate measurement of small-scale topographical elements can also be problematic (Bales and Wagner, 2009). Podhoranyi and Fedorcak (2015) presented an article that enlighten the error introduced by lidar-based elevation scanning due to the fact that the near-iR laser beam (1,064 nm) cannot penetrate water masses. Podhoranyi and Fedorcak (2015) compared two data sets of cross sections: real cross sections created from direct measurements of river channel and cross sections of the same river channel extracted from lidar. Inaccuracies between these two data sets impacted the results of the HEC-RAS simulation in the study area. Podhoranyi and Fedorcak (2015) concluded that inaccuracies introduced by lidar must be taken into account and must be corrected according to the catchment-specific conditions.

Chapter 3 - Methodology

3.1 Overview

The methodology outlined in this section provides improvements to hydraulic routing models through (i) developing reliable river cross sections approximations based on statistical analysis and information gathered from USGS streamflow measurement stations, (ii) linking the spatially distributed Noah Land Surface Model (Niu et al., 2011; David et al., 2009) to the Simulation Program for River Networks (SPRNT), and (iii) running the SPRNT hydraulic routing model based on the information gathered in the netlist (Hodges, 2013).

In terms of approximating river cross section geometries, this study presents a statistical approach, which is implemented, simulated, and compared to the results from USGS streamflow measurement stations. This approach, which is described in Section 3.3, is based on a statistical analysis given detailed channel cross section information for 25 USGS streamflow measurements stations across the Guadalupe and San Antonio River basins.

To run the SPRNT model the following actions were required: (i) the hydrological information from the study area was collected from the National Hydrography Dataset Plus Version 2, (ii) the cross section geometry, as well as the hydrological information, was incorporated into a standardize topographical representation, the netlist, which has been presented and discussed by Hodges (2013), and (iii) the model

runoff inputs were fed by the Noah Land Surface Model results (i.e. surface runoff and subsurface runoff) for every reach in the study river basin. The SPRNT model solves the full nonlinear Saint-Venant equations for one-dimensional unsteady flow and stage height in river channel networks with non-uniform bathymetry (Hodges, 2013).

3.2 Study Region

The San Antonio and Guadalupe River basins are located in south-central Texas. The Guadalupe River basin has a drainage area of 6700 square miles as well as about 3000 river and stream reaches, while the San Antonio River basin has a drainage area of 4180 square miles and about 2000 river and stream reaches. These river basins are chosen for study to determine future impacts of constructed infrastructure on flow dynamics, and based on the existence of previous hydrological studies done by David (2009); David et al. (2009). Figure 3 presents the Guadalupe and San Antonio River basins.

The San Antonio River basin is a dynamic ecosystem with rivers, creeks and streams that can quickly be impacted by rain events. This basin is bordered on the west by the Nueces River basin and on the east by the Guadalupe River basin. Average elevation of the basin is 229 meters; the lowest and the highest elevation are 2 and 710 meters (David, 2009). The Guadalupe River basin is the fourth largest river basin whose watershed area is entirely within Texas and is prone to severe flooding. The flow in the lower reaches is controlled by Canyon Dam (David, 2009).

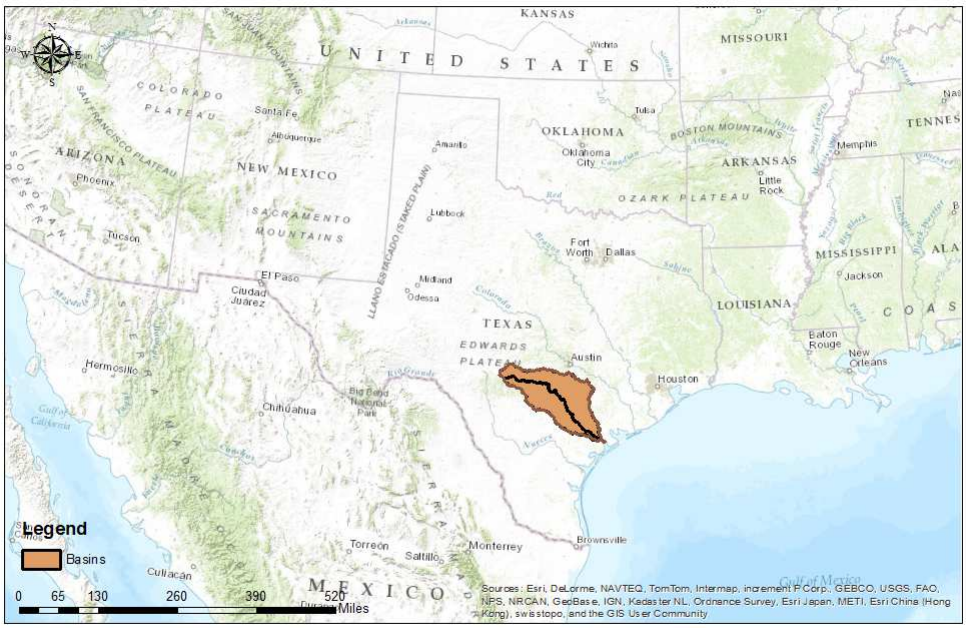

Figure 3: The Guadalupe and San Antonio River Basins

3.3 Statistical Hydraulic characterization - Trapezoidal Approximation

In the absence of comprehensive empirical data, it can be argued that simple form (i.e. trapezoidal, rectangular or parabolic) cross-sections are reasonable approximations for many channels. Indeed, as discussed in Section 2.2, prior models have adopted simpler rectangular channels for dynamic routing, and Orlandini and Rosso (1998) showed that rectangular cross sections, as opposed to rectangular shapes, can lead to considerable improvement in flow simulations.

The hypothesis for this analysis is that river cross sections in the Guadalupe and San Antonio River basins can be approximated as trapezoidal forms with symmetric side walls. Two parameters are required to specify a trapezoidal cross section: the bottom width (b_0), and the side wall slope (S_w, which is defined as the cotangent of the side wall angle with respect to the horizon). Figure 4 illustrates a trapezoidal cross section and its parameters.

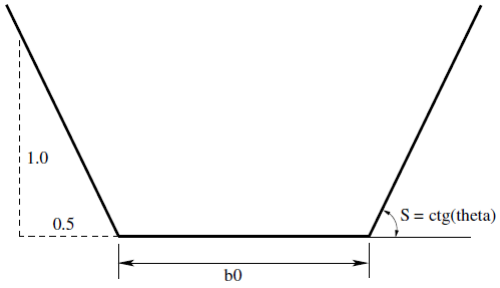

Figure 4: Trapezoidal cross section

Additionally, the hypothesis considers that the river cross section shape param-

eters (i.e. b_0 and S_w) present a relationship with the drainage area of the different streams in the study area. Given these two hypothesis, and knowing the drainage area for every stream in the study area, trapezoidal river cross sections can be approximated for every stream in the study area.

In the Guadalupe and San Antonio River basins there are 96 USGS streamflow measurement stations. 32 out of these 96 stations are inactive. From the 64, 13 are located along the Guadalupe River, 9 in the San Antonio River, 6 in the Medina River, and the rest in other (minor) rivers. Figure 5 presents the active USGS streamflow measurement stations in the study area.

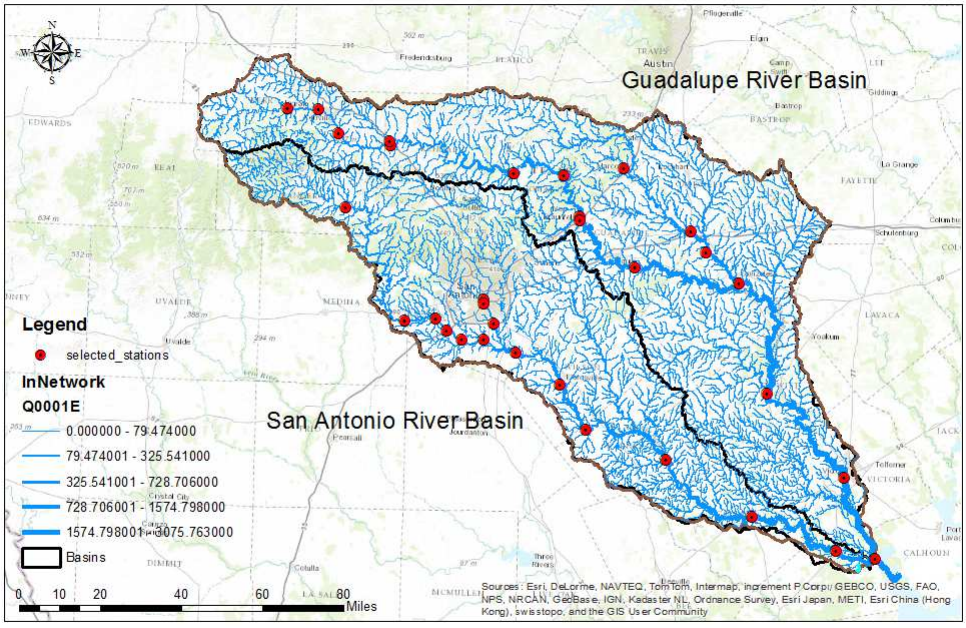

Figure 5: Study area and USGS streamflow measurement stations

Key elements of river channel cross section measured by the USGS and useful for

this study are:

- Channel cross-sectional area - A (ft^2)
- Channel top width - w (ft)
- Channel velocity - v (ft/s)
- Channel streamflow - Q (ft^3/s)
- Stage height - h (ft)

Stage height (h) is plotted vs. channel top width (w) for all the available stations in the study area to analyze the relationship between these to variables (i.e. linear, constant, exponential, power law). The relationship between h and w provides insight on the cross section geometry. For example, a constant relationship between these two variables would tacitly imply that the cross section can be approximated to a rectangular shape. A linear relationship would imply that the cross section can be approximated to a rectangular or trapezoidal shape.

The stage height vs. channel top width plots were analyzed to identify the correlation between the variables h and w. All of the measures of correlation ρ have the characteristic of being dimensionless and scaled to lie in the range $-1 \leq \rho \geq 1$. When $\rho = 0$, the data are said to be uncorrelated (Maidment, 1993). The Kendall's Correlation Coefficient τ and Kendall's test were used to quantify and test the strength of the correlation between the variables h and w in all the USGS stations. The null hypothesis H_0 for the Kendall's test is that the distribution of w does not change as

a function of h (i.e. there is no trend/correlation/monotonic relationship between the variables). The Kendall's test was performed as follows:

- The n data pairs $(h_1, w_1), (h_2, w_2), , (h_n, w_n)$ are indexed according to the magnitude of the h value, such that $h_1 h_2 h_n$ and w_i is the dependent variable value that corresponds to h_i.

- Examine all $n(n-1)/2$ ordered pairs of w_i values. Let P be the number of cases where $h_i > h_j (i > j)$ and let M be the number of cases where $h_i < h_j (i > j)$.

- Define the Kendall test statistics $S = P - M$.

- For $n > 10$, the test is conducted using a normal approximation. The standardized test statistic Z is computed as:

$$Z = \begin{cases} \frac{S-1}{\sqrt{Var(S)}} & \text{if } S > 0, \\ 0 & \text{if } S = 0, \\ \frac{S+1}{\sqrt{Var(S)}} & \text{if } S < 0. \end{cases} \tag{10}$$

  where

$$Var(S) = \frac{n(n-1)(2n+5)}{18} \tag{11}$$

- The null hypothesis is rejected at significance level α if $|Z| > Z_{1-\alpha/2}$, where $Z_{1-\alpha/2}$ is the value of the standard normal distribution with a probability of exceedance of $\alpha/2$. If the null hypothesis is rejected (H_0 = no trend), then there is trend/correlation/monotonic relationship between the variables (h and

w).

- The Kendall correlation coefficient τ is defined as:

$$\tau = \frac{S}{\frac{n(n-1)}{2}} \tag{12}$$

  Given that τ is a correlation coefficient, it can only take on values between -1 and 1, its sign indicates the sign of the slope of the relationship, and the absolute value indicates the strength of the relationship.

Kendall's test allows us to recognize monotonic relationships between the stage height (h) and channel top width (w). Based on the hypothesis for this first analysis (trapezoidal river cross sections), and the requirement for a specific type of relationship between the variables (linear), the Pearson Correlation Coefficient test was performed to assess the linearity of the relationship. The Pearson correlation coefficient r measures the linear association between two variables. As with Kendall's τ, Pearson's r can form a statistical test of independence. The null hypothesis (H_0) for this test is that the channel top width is independent and identically distributed normal random variables, not dependent on the stage height. Pearson's r is defined as:

$$r = \frac{S_{xy}}{\sqrt{S_{xx}S_{yy}}} \tag{13}$$

where S_{xx} is the variance of the stage height, S_{yy} is the variance of the channel top width, and S_{xy} is the co-variance between the stage height and channel top width. The test statistic t for the Pearson test is defined:

$$t = \frac{r\sqrt{n-1}}{\sqrt{1-r^2}} \tag{14}$$

The null hypothesis is rejected (i.e. there is no linear relationship between the variables h and w) if $|t| > t_{crit}$, where t_{crit} is the point on the Student's t distribution with $n-2$ degrees of freedom that has a probability of exceedance of $\frac{\alpha}{2}$.

Results of the Pearson correlation coefficient test show the USGS stations that present a linear relationship between the stage height and channel top width. The river cross section shape of these station can be approximated to a trapezoidal or triangular form.

Finally, to estimate the parameters that define a trapezoidal cross section (b_0 and S_w) and to describe the variation in the dependent variable (w), the ordinary least squares linear regression model was conducted. This linear regression model is defined as:

$$y_i = \beta_0 + \beta_1 \times \chi + \epsilon_1 \tag{15}$$

where y_i is the i^{th} observation of the response (or dependent) variable (in our case the channel top width), x_i is the i^{th} observation of the explanatory variable (the stage height), b_0 is the intercept, b_1 is the slope, e_i is the random error of residual for the i^{th} observation, and n is the sample size. Estimation of the parameters of the model, b_0 and b_1, were calculated as:

$$b_1 = \frac{S_{xy}}{S_{xx}} \tag{16}$$

$$b_0 = \bar{Y} - b_1 \bar{X} \tag{17}$$

where S_{xx} is the variance of the stage height, S_{xy} is the co-variance between the stage height and channel top width, $\bar{Y}$ is the mean of channel top width, and $\bar{X}$ is the mean of the stage height. The t statistics test equation (14) was used to determine the significance of the estimated slope b_1. If it is not possible to reject the null hypothesis for this test (H_0 is $b_1 = 0$), then the regression model should not be used, and the sample mean of the dependent variable (w) should be considered the best estimate of the channel width (rectangular approximation).

As seen from Figure 6, for a trapezoidal cross section approximation, the intercept (b_0) can be approximated to the bottom width of the river channel, and the slope (b_1) can be approximated as two time the side wall slope (S_w).

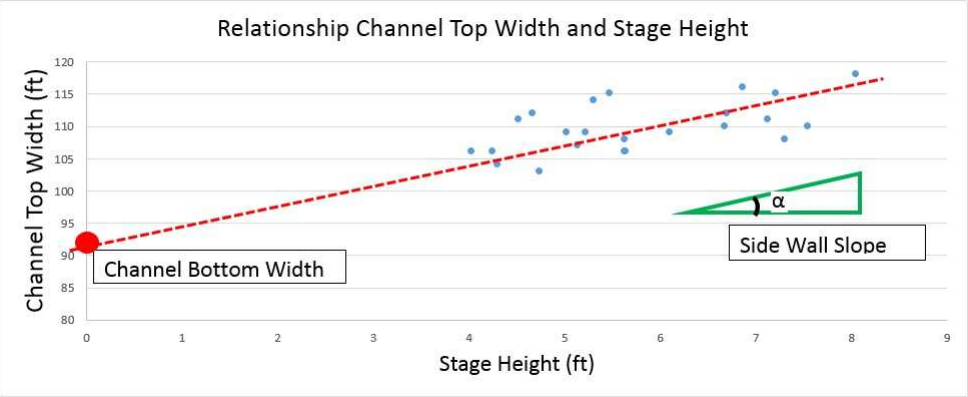

Figure 6: Trapezoidal cross section parameters for USGS station at Guadalupe Rv at New Braunfels

To complete the ordinary least squares linear regression, the residuals of the regression model were computed as:

$$e_(i) = y_1 - b_0 - b_1 \times \chi_i \tag{18}$$

A Probability Plot Correlation Coefficient (PPCC) test is performed for the residuals to assess the normal distribution assumption at a 10 % significance level. The Pearson correlation coefficient (r) is calculated as:

$$r = \frac{\sum_i (a_i - \bar{a})(w_i - \bar{w})}{\sqrt{\sum_i (a_i - \bar{a})^2 \times \sum_i (w_i - \bar{w})^2}} \tag{19}$$

where a_i are the observed residuals, $\bar{a}$ is the average of the observed residuals, w_i are the fitted quantiles, and $\bar{w}$ is the average of the fitted quantiles. The residuals of all the models are expected to have a normal distribution. After calculating the Pearson correlation coefficient (r), we compare the result with a lower critical value of the PPCC test (reference r with 5 % of significance level and n as the sample number for our study case). For our study Bloms plotting position will be used. The lower critical r value can be obtained from Table 8.3.3 from the Handbook of Hydrology (Maidment, 1993).

3.4 Model Framework Description

The National Hydrography Dataset of the United States has been synthesized into a geospatial dataset called NHDPlus which is referenced to a spheroidal Earth and has vector coverage for catchments and river reaches (David, 2009). The NHD-

Plus contains a GIS dataset that links the National Hydrography Dataset description of the mapped streams and water bodies of the nation with small catchments delineated around each stream reach. Each reach and its catchment are assigned a unique identifier, the COMID, and all features and attributes to this reach are labeled similarly. Additionally, the NHDPlus includes diverse attributes/fields such as FromNode, ToNode, divergence, network connectivity, stream order, slope, length, and mean annual flow.

Within our model framework, the core physical model governing the one-dimensional (1D) vertical fluxes of energy and moisture is the Noah Land Surface Model (LSM). This model simulates the overland flow routing as a fully unsteady, explicit, finite difference, one-dimensional diffusive wave flowing over the land surface. Sub-surface flow (down to 2-m depth) is also explicitly modeled using a quasi-steady state saturated flow model adapted from Wigmosta et al. (1994). The horizontal flow into a stream network calculated by Noah is the sum of surface and sub-surface runoff. The Noah LSM does not consider flow from the stream back to the landscape or aquifer.

In this study, similar to previous studies (David, 2009), the NHDPlus dataset is used as the land base for the SPRNT model as well as for the Noah LSM. Figure 7 shows three components of the geospatial framework used in this study

Finally, all the information will be gathered in the netlist. The netlist is a format used to describe river network topology. It was used earlier for electric circuit topology. The idea and objective of the netlist is to standardize topographical rep-

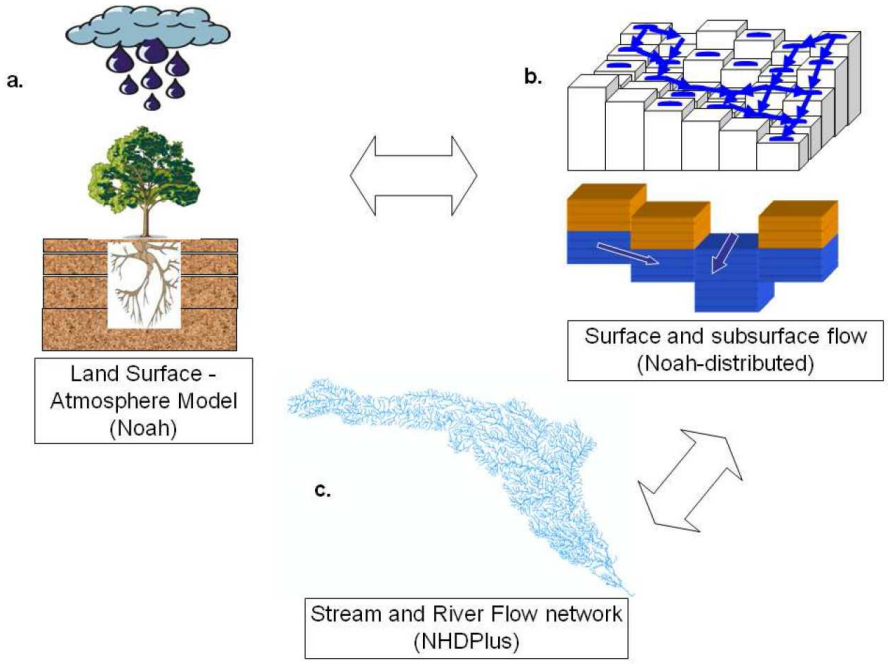

Figure 7: Noah Model and NHDPlus information (David, 2009)

resentation and make changing between different river network models a simpler process (Hodges, 2013; Liu, 2012).

A netlist syntax for river network topology has been developed using ideas from VLSI design. Our river netlist is organized using a set of defined blocks. Typically defined within a block is either a segment (river reach), a computational node (connection between two reaches), or a junction (connection between multiple reaches). Additional a block includes the river cross-section shape, length of the computational element, and flow resistance coefficient (Manning's n). Additional blocks are used to define the upstream boundary conditions, downstream boundary conditions, and lateral inflows (Liu, 2012). A simple example netlist is provided in the appendix.

Furthermore, within the SPRNT model, a topographical checker is implemented to analyze network continuity using a network graph and a depth-first-search (DFS) algorithm. The topographical checker also ensures boundary conditions are defined for extreme upstream and downstream nodes (Liu, 2012). If the netlist presents unconnected reaches or lacks boundary conditions the network fails the topographical checking and the SPRNT does not run a simulation.

Chapter 4 - Results and Discussion

4.1 Trapezoidal Cross Section Approximation

Table 1 shows the USGS streamflow measurement stations used for this study as well as the time period of the data and the drainage area for each station. As seen in Table 1, the data was collected trying to maintain the same Rating Curve (RC) number for each station. The Rating Curve is a relationship between stage height and channel discharge at a cross section of a river, and usually defines the shape of the cross section. Thus, collecting data with different RC numbers would imply different shapes of cross sections.

Station Name	# Obs	Time Period	# RC	D. Area(mi^2)
Guadalupe Rv at Tivoli	20	2007-2010	2	10128
Guadalupe Rv at Bloomington	22	2010-2012	1	5816
Guadalupe Rv at Victoria	25	2007-2010	19	5198
Guadalupe Rv at Gonzales	23	2007-2010	5	3490
Guadalupe Rv at FM117	27	2007-2010	2	1957
Guadalupe Rv at New Braunfels	24	2007-2010	9	1518
Guadalupe Rv at Spring Branch	18	2010-2011	16	1315
Guadalupe Rv at Comfort	20	2008-2010	25	839
Guadalupe Rv at Center Point	18	2008-2010	1	553
Guadalupe Rv at Kerville	18	2008-2010	7	494
Guadalupe Rv at Hunt	17	2007-2009	8	169
San Antonio Rv at McFaddin	21	2008-2011	2,3	4134
San Antonio Rv at Goliad	20	2008-2010	17,18	3921
San Antonio Rv at Floresville	20	2009-2011	4	1964
San Antonio Rv at Elmendorf	21	2009-2012	16	1743
San Antonio Rv at Loop 410	23	2008-2010	8	125
Medina Rv at San Antonio	24	2007-2010	21,22	1317

Table 1: USGS streamflow measurement stations in the study area

Figure 8 presents channel top width vs. stage height for different USGS stream-

flow measurement stations, and Table 2 shows the Kendall's correlation coefficient (τ), Pearson's correlation coefficient (r), and its p-values.

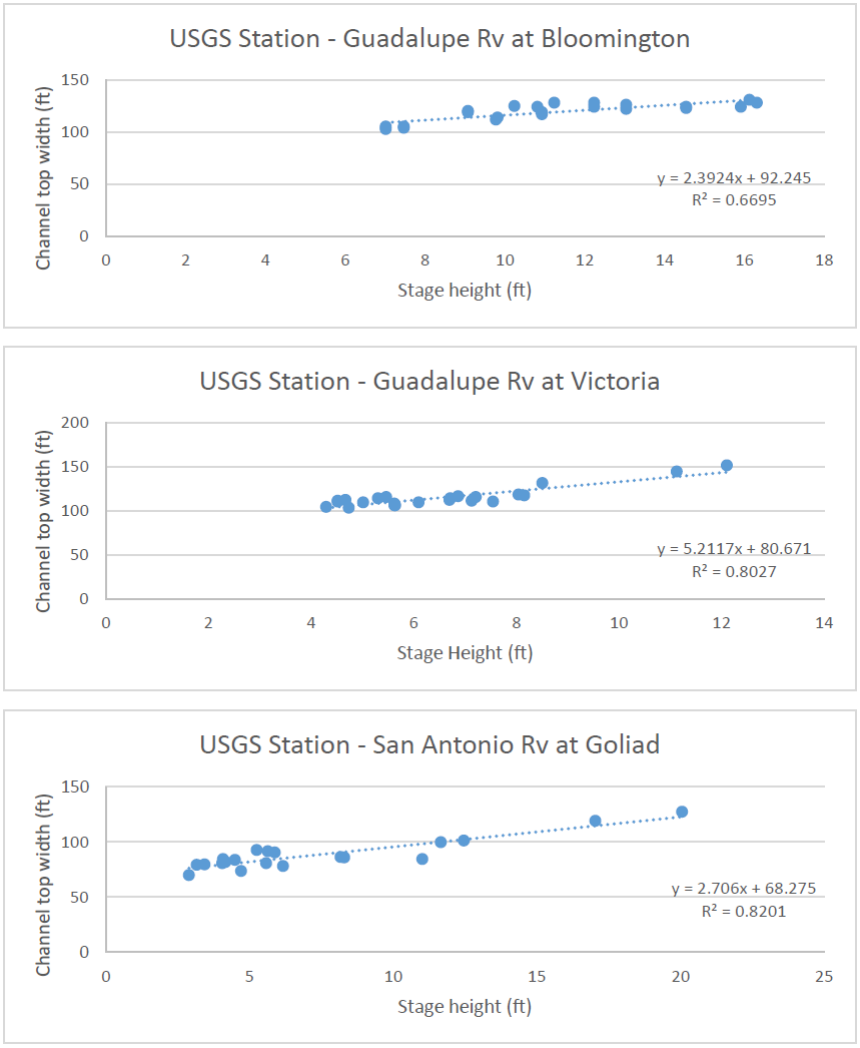

Figure 8: Channel top width vs. Stage height for different USGS stations in the study area

As stated in Section 3.3, the Kendall correlation coefficient τ as well as the Pearson correlation coefficient demonstrate the monotonic relationship and correlation between the examined variables. The p-values or probability values are relatively small (i.e. p-value ≤ 0.05), which show a strong evidence on the study hypothesis that the channel top width and stage height are correlated.

Station Number	τ	p-value	r	p-value
Guadalupe Rv at Tivoli	0.32	0.049	0.55	0.012
Guadalupe Rv at Bloomington	0.63	4.53e-05	0.82	3.27e-06
Guadalupe Rv at Victoria	0.61	1.76e-05	0.96	3.76e-14
Guadalupe Rv at Gonzales	0.71	1.59e-06	0.96	1.62e-13
Guadalupe Rv at FM117	0.73	9.71e-08	0.88	2.3e-09
Guadalupe Rv at New Braunfels	0.75	2.82e-07	0.91	4.72e-10
Guadalupe Rv at Spring Branch	0.23	0.16	0.42	0.085
Guadalupe Rv at Comfort	0.71	1.13e-05	0.73	0.00025
Guadalupe Rv at Center Point	0.38	0.027	0.43	0.075
Guadalupe Rv at Kerville	0.63	0.0001	0.62	0.0035
Guadalupe Rv at Hunt	0.61	0.0004	0.61	0.0066
San Antonio Rv at McFaddin	0.75	1.83e-06	0.92	3.12e-09
San Antonio Rv at Goliad	0.59	0.00024	0.91	4e-08
San Antonio Rv at Floresville	0.41	0.012	0.923	6.14e-09
San Antonio Rv at Elmendorf	0.15	0.31	0.76	7.39e-05
San Antonio Rv at Loop 410	0.49	0.0009	0.84	4.98e-07
Medina Rv at San Antonio	0.79	5.12e-08	0.95	1.35e-14

Table 2: Kendall and Pearson correlation coefficients

Following this study's hypothesis (correlation and linear relationship between the channel top width and stage height), Table 3 presents the linear regression results and parameters for the trapezoidal cross sections approximation and the t test of significance of b_1.

As seen from Table 3, b_0 represents the channel bottom width of the trapezoidal approximation, while b_1 represents the channel side wall slope. As stated in Section 3.3, if it is not possible to reject the null hypothesis that $b_1 \neq 0$ then the regression model should not be used, and the sample mean of the channel top width should be considered as the best estimate for the channel bottom width. As an approximation, a regression coefficient is significant if the absolute value of its t statistic is greater

Station Number	b_0	b_1	t
Guadalupe Rv at Tivoli	117.9	0.98	2.8
Guadalupe Rv at Bloomington	92.2	1.19	6.36
Guadalupe Rv at Victoria	82.4	3.16	16.34
Guadalupe Rv at Gonzales	58.2	2.88	16.53
Guadalupe Rv at FM117	45.2	4.56	9.1
Guadalupe Rv at New Braunfels	51.03	13.9	10.52
Guadalupe Rv at Spring Branch	50.5	4.48	1.90
Guadalupe Rv at Comfort	29.1	5.83	4.53
Guadalupe Rv at Center Point	18.7	5.61	1.91
Guadalupe Rv at Kerville	43.5	15.82	3.36
Guadalupe Rv at Hunt	42.4	16	3.11
San Antonio Rv at McFaddin	61.1	0.99	10.32
San Antonio Rv at Goliad	68.3	1.35	9.1
San Antonio Rv at Floresville	29.6	1.33	10.24
San Antonio Rv at Elmendorf	17.18	1.32	5.03
San Antonio Rv at Loop 410	23.52	2.17	7.12
Medina Rv at San Antonio	15.20	4.27	15.9

Table 3: Linear Regression Parameters

than 2, that is $t < -2$ or $t > 2$ (Maidment, 1993).

Following the downstream hydraulic geometry approach, and to identify any potential relationship between the trapezoidal parameters approximations and the study area, Table 4 compiles the drainage area for the USGS streamflow measurement stations and the cross section parameters for each of the USGS stations.

Figures 9 and 10 present the channel bottom width vs. drainage area, as well as channel side wall slope vs. drainage area plots. With the information provided in Figures 9 and 10, correlation coefficients tests as well as a regression model were performed to identify any potential trends.

Station Number	b_0	b_1	Drainage area (sq mi)
Guadalupe Rv at Tivoli	117.9	0.98	10128
Guadalupe Rv at Bloomington	92.2	1.19	5816
Guadalupe Rv at Victoria	82.4	3.16	5198
Guadalupe Rv at Gonzales	58.2	2.88	3490
Guadalupe Rv at FM117	45.2	4.56	1957
Guadalupe Rv at New Braunfels	51.03	13.9	1518
Guadalupe Rv at Spring Branch	50.5	4.48	1315
Guadalupe Rv at Comfort	29.1	5.83	839
Guadalupe Rv at Center Point	18.7	5.61	553
Guadalupe Rv at Kerville	43.5	15.82	494
Guadalupe Rv at Hunt	42.4	16	169
San Antonio Rv at McFaddin	61.1	0.99	4134
San Antonio Rv at Goliad	68.3	1.35	3921
San Antonio Rv at Floresville	29.6	1.33	1964
San Antonio Rv at Elmendorf	17.18	1.32	1743
San Antonio Rv at Loop 410	23.52	2.17	125
Medina Rv at San Antonio	15.20	4.27	1317

Table 4: Relationship between cross section parameters and drainage area

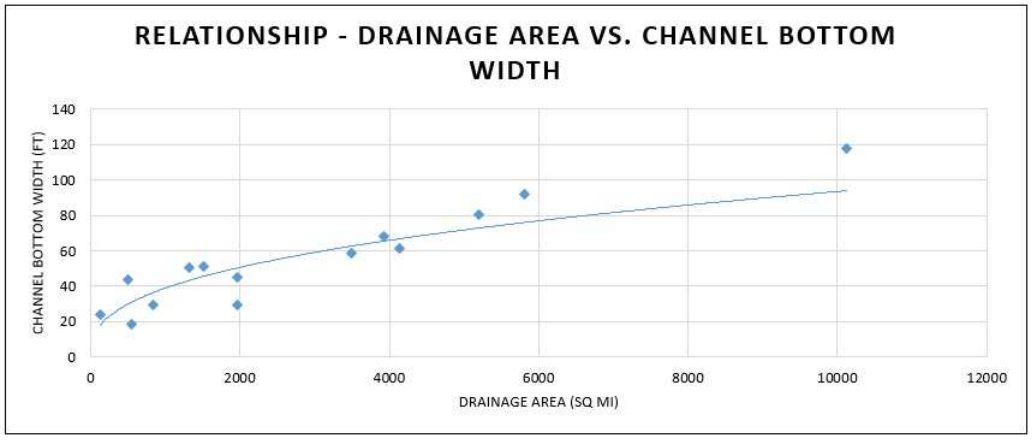

Figure 9: Relationship between channel bottom width vs. drainage area

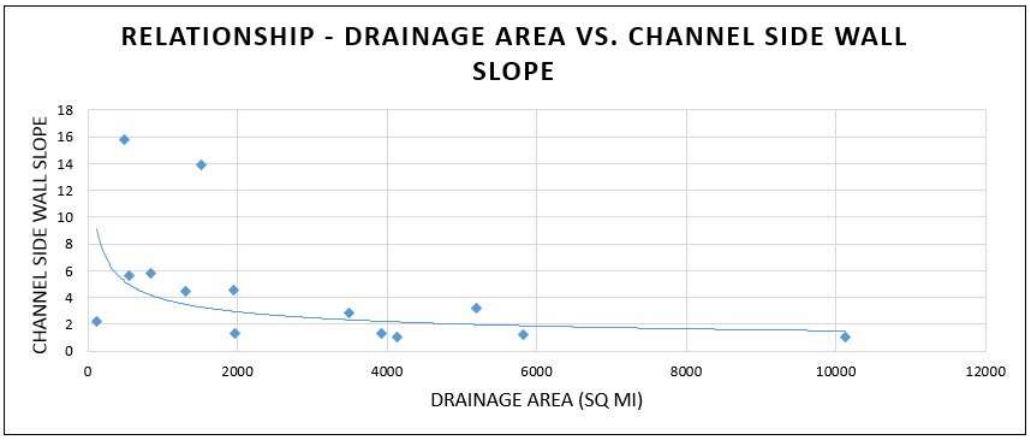

Figure 10: Relationship between channel side wall slope vs. drainage area

Given the scale and nature of the variables (i.e. trapezoidal cross sections approximations and drainage area), and following the work of Leopold and Maddock (1953), a logarithmic transformation is performed and the results are presented in Table 5 and Figures 11 and 12.

Station Number	b_0	b_1	Drainage area (sq mi)
Guadalupe Rv at Tivoli	2.07	0	4.01
Guadalupe Rv at Bloomington	1.96	0.08	3.76
Guadalupe Rv at Victoria	1.9	0.49	3.71
Guadalupe Rv at Gonzales	1.79	0.45	3.54
Guadalupe Rv at FM117	1.65	0.65	3.29
Guadalupe Rv at New Braunfels	1.71	1.14	3.18
Guadalupe Rv at Spring Branch	1.70	0.65	3.11
Guadalupe Rv at Comfort	1.46	0.77	2.92
Guadalupe Rv at Center Point	1.27	0.74	2.74
Guadalupe Rv at Kerville	1.64	1.19	2.69
San Antonio Rv at McFaddin	1.78	0	3.62
San Antonio Rv at Goliad	1.83	0.13	3.59
San Antonio Rv at Floresville	1.47	0.12	3.29
San Antonio Rv at Loop 410	1.37	0.33	2.09

Table 5: Logarithmic transformation for cross section parameters and drainage area

The Kendall and Pearson correlation coefficient tests were calculated for the logarithmic transformation values from Table 5 and Figures 11 and 12. Additionally,

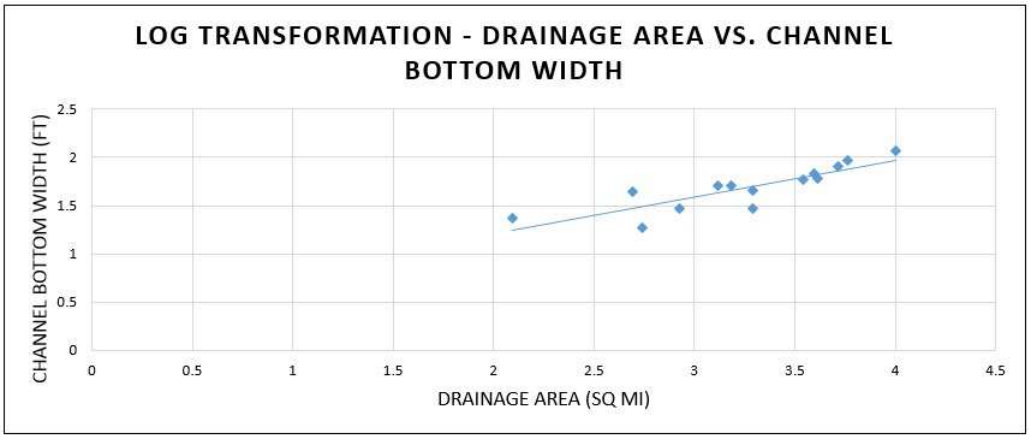

Figure 11: Logarithmic transformation for cross section parameters and drainage area

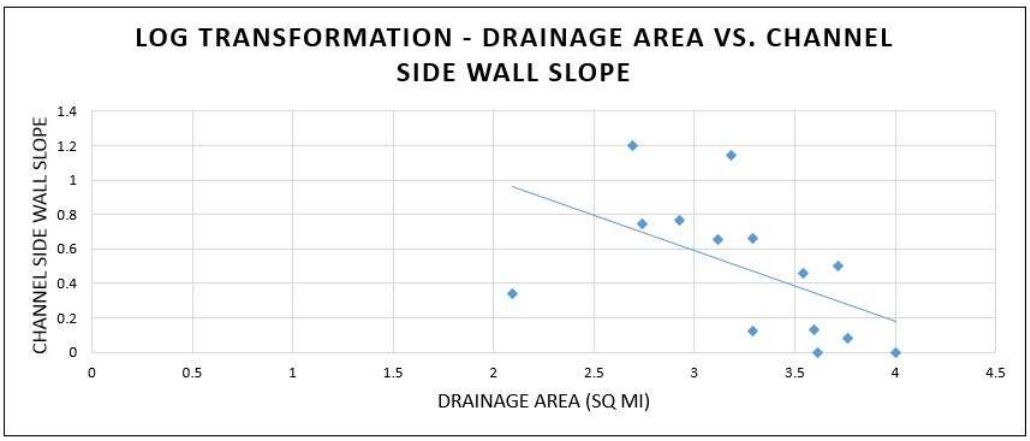

Figure 12: Logarithmic transformation for cross section parameters and drainage area

a linear regression model was performed for the logarithmic transformation values. Results of the correlation coefficient test as well as from the linear regression model are presented in Table 6.

Parameter	τ	p-value	r	p-value	intercept	slope	t
Channel bottom width	0.78	0.0001	0.85	9.97e-05	0.44	0.382	5.69
Channel side wall slope	-0.55	0.0059	-0.52	0.052	1.82	-0.41	-2.15

Table 6: Results for logarithmic transformation of relationship between cross section parameters and drainage area

Then, the equations for determining the channel bottom width and channel side wall slope for the Guadalupe and San Antonio River basins are:

$$b_0 = 2.7 \times DA^{0.382} \tag{20}$$

$$b_1 = 65 \times DA^{-0.41} \tag{21}$$

where DA is the drainage area for the stream, and b_0 as well as b_1 are the trapezoidal cross section approximations.

4.2 SPRNT Simulation

In this section, the Guadalupe and San Antonio river basins simulation results are presented. Additionally to the trapezoidal cross section approximation for each stream in the study area, the SPRNT model requires boundary, initial conditions, channel roughness (S_f), and the bottom slope information (S_0). The parameter that was not calibrated was Mannings n with a constant value for each reach of 0.03. Mannings n value was adopted based on values for natural rivers presented by Chow

(1959).

For our river network, the principal boundary conditions are surface and sub-surface runoff that occur both at the ultimate headwater and along all the streams in the study area. As stated in Section 3.4, surface and sub-surface runoff is collected from the Noah LSM in units of mm/hr. The multiplication of the individual catchment area, in units of km^2, and the values of the LSM provide the discharge value along the stream in that particular catchment area. Table 7 and Figure 13 show the surface and subsurface values for a particular catchment area.

Time and Date	ComID	surface runoff
2010-01-01 00:00	1622713	0.05
2010-01-01 01:00	1622713	0.00
2010-01-01 02:00	1622713	0.025
...	...	...
2010-02-01 00:00	1622713	0.1
2010-02-01 01:00	1622713	0.1
2010-02-01 02:00	1622713	0.1
...	...	...
2010-06-01 00:00	1622713	0.0
2010-06-01 01:00	1622713	0.034
2010-06-01 02:00	1622713	0.018
...	...	...
2010-12-31 21:00	1622713	0.0
2010-12-31 22:00	1622713	0.01
2010-12-31 23:00	1622713	0.0

Table 7: Surface runoff for 1622713 stream, where the USGS Guadalupe Rv at Victoria station is located

The initial conditions for the water surface level (related to the area by the cross sectional shape) and flow rate are calculated from the steady state from the Saint-Venant equations and the Chezy-Maning equation.

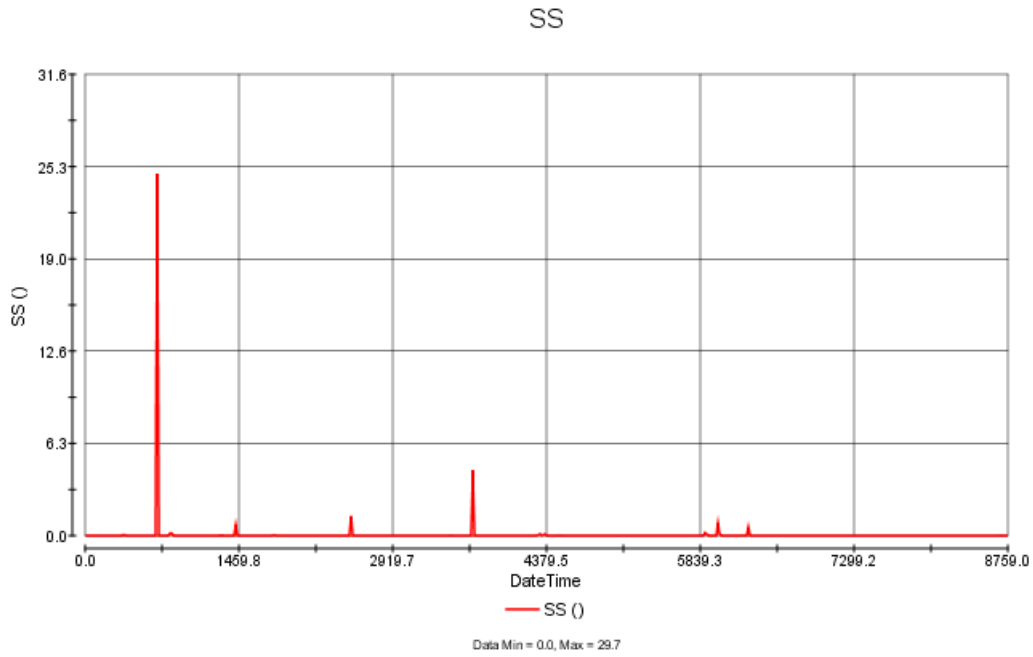

Figure 13: Surface runoff for 1622713 stream along the 2010

The information from the cross section, boundary conditions, initial conditions, channel roughness, and stream's bottom slopes is collected in the netlist, which was referenced in Section 3.4 and described in Liu (2012). Appendix A presents an example of a part of the netlist used for this study.

The SPRNT model is simulated for the 2010 year. Characteristics of the simulation are described in Table 8.

Parameter	Value
Time step	4 min
Duration	8760 hours
Reaches	5195
Computational nodes	67333
Reaches with qsource	1540
Lateral sources	28153
Print interval	6 hours

Table 8: SPRNT model parameters

Figures 14 and 15 show observed and simulated daily flow from January 2010 to December 2010 at the USGS streamflow measurement stations. In these figures, one can see the baseflow for each station as well as the peak flows generated by the lateral inflows/precipitation. Due to use of initial values from the steady state

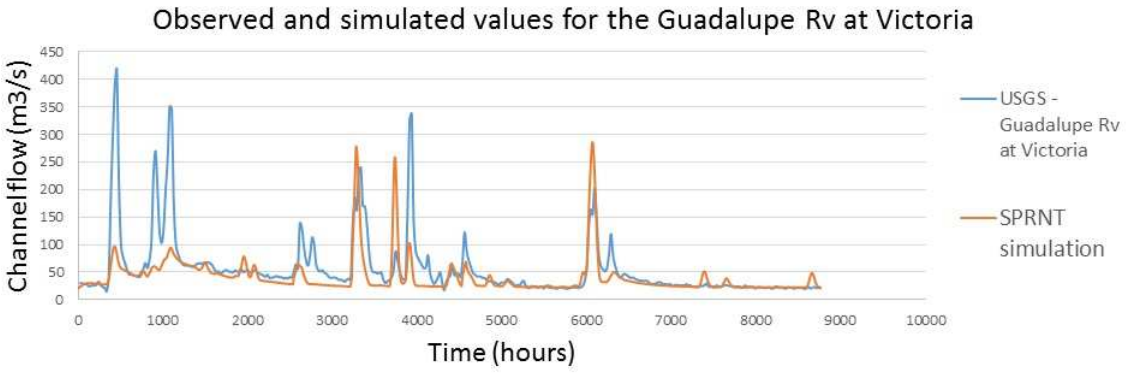

Figure 14: Observed and simulated channel discharges for Guadalupe Rv at Victoria

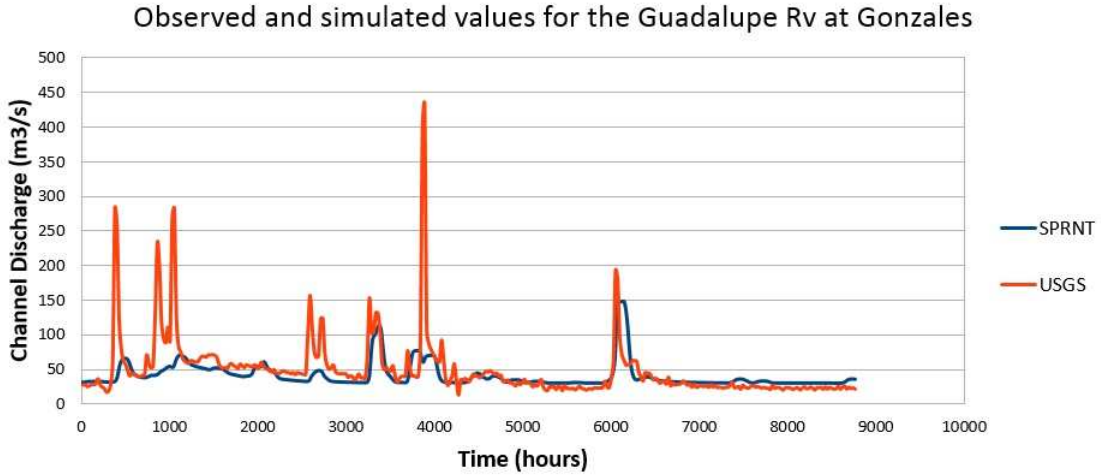

Figure 15: Observed and simulated channel discharges for Guadalupe Rv at Gonzales

Saint-Venant equations, the simulated results present a spin-up time, which is the time that requires the model to be no longer affected by the initial values or initial conditions. As seen from figures 14 and 15 the spin-up time is approximately from

3-4 months. where the peak flows are not well simulated. However, after the spin-up time, one can see a close agreement between peaks flows as well as baseflow for the USGS stations. Seasonal precipitation in this region causes alternated high and low water periods. Hydrographs of the upper part of the basin are noisy, with several peaks related to intense rainfall events. As the flood wave travels to the lower part of San Antonio and Guadalupe river basins, it is attenuated and delayed due to the storage of high volumes of water on the floodplain.

4.3 Discussion

One scenario is proposed for the study simulation: trapezoidal cross section approximation linked with runoff from the Noah LSM using the SPRNT hydraulic model. Correlation coefficient tests demonstrate the monotonic trend as well as the correlation for channel top width and stage height for the selected USGS streamflow measurement stations. Similarly, the linear regression model performed for the same variables detected a linear relationship between them.

Based on the linearity between the channel top width and stage height, the author assumes that there is potential for triangular or trapezoidal approximation for the river cross sections in the study area. As seen in Figure 6, when the stage height becomes zero, the intercept (b_0) becomes the channel bottom width. Similarly, the slope (b_1) of the linear relationship is related to the channel side wall slope (S_w).

Cross section parameters are related to the drainage area for every reach in the study area, based on downstream hydraulic geometry approach. Then, as presented in similar works (David, 2009; David et al., 2009), this work uses of NHDPlus as a hydrological layout as well as the use of the Noah LSM. Results for different stations along the Guadalupe river show: (i) trapezoidal cross section approximations can be used for areas where limited data is available, (ii) for large-scale river networks, the NHDPlus compiles the require information for hydraulic as well as for hydrological model, (iii) the use of Noah LSM seems to be in agreement with the results of this study,and (iv) SPRNT represents adequately hydrological features (e.g. channel discharge and water level) in a large-scale river network, even without calibration of Manning's n.

Chapter 5 - Conclusions and Future Work

5.1 Conclusions

This work describes the development of a methodology to approximate channel cross sections for large scale hydraulic modeling. Additionally, this research present a validation for the physically based large-scale hydraulic SPRNT model in the San Antonio and Guadalupe river basins. The model results are able to reproduce observed hydrographs at different spatial scale from the USGS streamflow measurement stations in the study area.

The model and methods used to derive the necessary information were tested in the San Antonio and Guadalupe river basins, which are located in central Texas. The case study shows the feasibility of downstream hydraulic geometry as well as regression models for cross section parameter extraction. A comparison between observed and simulated discharges and water levels at USGS streamflow measurement stations shows that the model is capable of reproducing the main hydrological features of the San Antonio and Guadalupe river basins. An important detail is that calibration of parameters related to the hydrodynamic model was not necessary.

However, while our cross section approximation for flow propagation in rivers is relatively complete, the description of floodplain dynamics is a continuation of the river description. Our approach does not fully reproduce what is actually happening in the floodplains.

Sources of model errors, which can be extrapolated to other similar large-scale models, were investigated by using model validation results. These errors may be related to input data (i.e. lateral inflows from the LSM, approximations in cross sections), and limitations of the hydraulic model itself. Nevertheless, results show that it is possible to employ fully dynamic hydraulic models within large-scale river networks even using limited data for river geometry.

5.2 Future Work

This work assessed trapezoidal cross section approximations. As mentioned in Section 2.3, there are software tools currently available to extract geospatial features such as channel cross sections for a river network. Future work should include simulations with other simpler cross sections approximations (rectangular, semi-circular) as well as cross sections extracted from DEM or lidar data with the sufficient resolution for the modeling purposes.

Additionally, for this research the Noah LSM uses a approximated grid cell of 12 km by 12 km. Currently, there are other Land Surface models, which operate in finer grid which would mean an upgrade for boundary conditions into the model. Moreover, a weighted method should be incorporated for multiplying catchment areas and the runoff values based on the portion of catchment area located in the grid.

Finally, a calibration process should be conducted for the SPRNT model to determine adequate channel roughness parameters.

Appendix A

This appendix shows all the python scripts used to prepare and pre-process the input data for the SPRNT hydraulic routing model. The comments explaining of each module is presented with a # in front of the code.

Python Script 1: Multiply Catchment Area and Runoff valued from Noah-MP LSM

```
#---------------------------------------
# Name:        Multiplication
# Purpose:    Multiply the LSM values and Drainage Area
#
# Author:      Alfredo Hijar
#
# Created:     12/11/2014
# Copyright:   (c) Alfredo 2014
#---------------------------------------

def main():
    pass
if __name__ == '__main__':
    main()
import csv

# read the values of the LSM model
file000 = open('lsm.txt','r')
row=[]
for s in file000.readlines():
    column=[]
    line=s.split()
    for field in line: column.append(field)
    row.append(column)
file000.close

# read the values of the drainage area
file001 = open('area.txt','r')
row1=[]
for r in file001.readlines():
```

```
    column1=[]
    line1=r.split()
    for field in line1: column1.append(field)
    row1.append(column1)
file001.close

# Multiply the values
for i in range(len(row)):
    for j in range(len(row1)):
        if row[i][2] == row1[j][0]:
            row[i][3]= int(row[i][3])*int(row1[j][1])
#print row

# Create new file with the multiplied values
new=open('output2.txt','w')
for i in (row):

    k='   '.join([str(j) for j in i])
    print k
    new.write(k+'\n')
new.close
```

Python Script 2: Convert the CSV files to NetCDF Format

```
# main_opt.py
# This module converts the csv files containing the LSM information,
# as well as the drainage area information into netcdf format.

import sys
from netCDF4 import Dataset
from numpy import array

# Specifi the number of time and point steps for the model.
# In this case, there are 5288 reaches and 1 month of simulation.
POINTS_PER_STEP = 5288
TIMESTEPS = 31 * 24


def read_chunk(file_handle, n_lines=POINTS_PER_STEP):
    raw_lines = [file_handle.next() for x in xrange(n_lines)]
    parsed_lines = [line[:-2].split(",") for line in raw_lines]
    return array([float(record[2]) for record in parsed_lines])


def read_first_chunk(file_handle, n_lines=POINTS_PER_STEP):
    raw_lines = [file_handle.next() for x in xrange(n_lines)]
    parsed_lines = [line[:-2].split(",") for line in raw_lines]
    data = array([float(record[2]) for record in parsed_lines])
    comids = [int(record[1]) for record in parsed_lines[:n_lines]]
    return comids, data


if __name__ == "__main__":

    if len(sys.argv) < 5:
        sys.exit("Please enter the name of the files."
                 " First the sub-surface and then the surface file.")

    bgs_filename = sys.argv[1]
    ss_filename = sys.argv[2]
    output_file = sys.argv[3]
    TIMESTEPS = int(sys.argv[4])

    bgs_file = open(bgs_filename, 'r')
    ss_file = open(ss_filename, 'r')

    ncfile = Dataset(output_file, 'w', format='NETCDF4_CLASSIC')
```

```
    ncfile.createDimension('COMID', POINTS_PER_STEP)
    ncfile.createDimension('DateTime', TIMESTEPS)

    ncfile.createVariable('COMID', 'i4', dimensions=('COMID'))
    ncfile.createVariable('BGS', 'f4', dimensions=('DateTime', 'COMID'))
    ncfile.createVariable('SS', 'f4', dimensions=('DateTime', 'COMID'))

    # throw away the first line
    bgs_file.readline()
    ss_file.readline()

    # Setup bgs shape
    bgs_var = ncfile.variables['BGS']
    ss_var = ncfile.variables['SS']

    comids, chunk0_bgs = read_first_chunk(bgs_file)
    comids, chunk0_ss = read_first_chunk(ss_file)
    bgs_var[0] = chunk0_bgs
    ss_var[0] = chunk0_ss

    for x in xrange(1, TIMESTEPS-1):
next_chunk_bgs = read_chunk(bgs_file)
bgs_var[x] = next_chunk_bgs
next_chunk_ss = read_chunk(ss_file)
ss_var[x] = next_chunk_ss

    # Save the comids
    comid_var = ncfile.variables['COMID']
    comid_var[:] = comids
    ncfile.close()
```

Python Script 3: Statistical tools for correlation coefficients and regression models

```
import pandas
import scipy.stats as stats
import math

colnames = ['height', 'width']
data = pandas.read_csv('csv_sws.csv', names=colnames)

height = list(data.height)
width = list(data.width)
slope, intercept, r_v, p_v, std_e = stats.linregress(height,width)
tau, p_value_2 = stats.kendalltau(height, width)
pearson_r, p_value_3 =  stats.pearsonr(height, width)
n = len(width)
t = pearson_r*math.sqrt(n-2)/(math.sqrt(1-pearson_r**2))
sws = slope/2
print tau
print p_value_2
print p_value_1
print "r-squared:", r_value**2
print r_value
print pearson_r
print p_value_3
print slope
print intercept
print t
```

Netlist Example

```
1 ## automatically generated by a translation script
2 ## on Jul 12 2013 15:46:33 CDT
3 ## one segment river bed , test the mixture of xy and trap x- section
4 ## start from base flow 1 and spin down
5
6 def options metric =1 end
7 def options epoch =2013 -12 -02 T02 :30:00 Z end
8 def options TimeStep =60 TimeStepUnit = second end
9 def options PrtInterval =2 PrtIntervalUnit = minute end
10 def options PrtQ =1 PrtA =1 PrtDepth =1 PrtSurfElev =1 PrtCoord = 1
11 end
12 def node id= node_1 sr =0.0083 n =0.04 zr =707.23 hr =0.0
13 xcoord =123.45 ycoord =567.89 def xy
14 x =0.0 y =6.0
15 x =2.5 y =1.0
16 x =3.5 y =1.0
17 x =6.0 y=6
18 end
19 end
20
21 def node id =2 sr =0.0083 n =0.04 zr =707.23 hr =0.0
22 def trapezoidal
23 BottomWidth =1 slope =0.5
24 end
25 end
26
27 def node id =3 sr =0.0083 n =0.04 zr =707.23 hr =0.0
28 def xy
29 x =0.0 y =6.0
30 x =2.5 y =1.0
31 x =3.5 y =1.0
32 x =6.0 y=6
33 end
34 end
35
36 def node id =4 sr =0.0083 n =0.04 zr =707.23 hr =0.0
37 def trapezoidal
38 BottomWidth =1 slope =0.5
39 end
40 end
41
42 def node id =5 sr =0.0083 n =0.04 zr =707.23 hr =0.0
43 def xy
```

```
44 x =0.0 y =6.0
45 x =2.5 y =1.0
46 x =3.5 y =1.0
47 x =6.0 y=6
48 end
49 end
50
51 def node id =6 sr =0.0083 n =0.04 zr =707.23 hr =0.0
52 def xy
53 x =0.0 y =6.0
54 x =2.5 y =1.0
55 x =3.5 y =1.0
56 x =6.0 y=6
57 end
58 end
59
60
61 def segment up= node_1 down =2 Length =40 end
62 def segment up =2 down =3 Length =40 end
63 def segment up =3 down =4 length =40 end
64 def segment up =4 down =5 length =40 end
65 def segment up =5 down =6 length =40 end
66
67 def qsource
68 location = node_1
69 def TimeSeries
70 TimeUnit = minute
71 t=0 v =1.0
72 t=1 v =1.0
73 t=2 v =0.5
74 t=4 v =0.1
75 t=6 v =0.5
76 t =80 v =0.1
77 t =100 v =0.1
78 t =1000 v =0.1
79 t =1200 v =0.5
80 t =1400 v =1.0
81 t =2500 v =1.0
82 t =5000 v =1.0
83 end
84 end
85
86
87 def BoundaryCondition
88 location =6 type = area
```

```
89 def timeseries
90 TimeUnit = minute
91 t=0 v=1
92 t =2800 v=1
93 end
94 end
95
96 def options
97 StopTime =8 StopTimeUnit = minute
98 end
99
100 ## end
```

References

Ackers, P. (1964). Experiments on small sstream in alluvium. *Proceedings of the American Society of Civil Engineering 90*, 1–37.

Bales, J. and C. Wagner (2009). Sources of uncertainty in flood inundation maps. *Journal Flood Risk Management 2*, 139–147.

Brush, L. (1961). Drainage basins, channels and flow characteristics of selected sstream in central Pennsylvania. *USGS Professional Paper 282*, 1–11.

Buhman, D., T. Gates, and C. Watson (2002). Stochastic variability of fluvial hydraulic geometry: Mississippi and red rivers. *Journal of Hydraulic Engineering 128*, 426–437.

Chang, H. (1988). *Fluvial PrProcess in River Engineering*. Wiley.

Chong, S. (1970). The width, depth, and velocity of Sungei Kimla, Perak. *Geographica 6*, 63–72.

Chow, V. T. (1959). *Open Channel Hydraulic*. McGraw Hill.

Cook, A. and V. Merwade (2009). Effect of topographic data, geometric configuration and modeling approach on flood inundation mapping. *Journal of Hydrology 377*, 131–142.

David, C. (2009). *Towards river flow computation at the continental scale*. Ph. D. thesis, University of Texas at Austin.

David, C., D. Gochis, D. Maidment, W. Yu, and D. Yates (2009). Using NHDPlus as the Land Base for the Noah-distributed model. *Transactions in GIS 13*, 363–377.

de Saint-Venant, B. (1871). Theorie du mouvement nonpermanent des eaux avec application aux crues des rivieres et a lintroduction des marees dans leur lit. *Comptes Rendus Acad. Sci. Paris 73*, 147–154.

Ferguson, R. (1986). Hydraulic and hydraulic geometry. *Progress in Physical Geography 10*, 1–31.

Gichamo, T. Z., I. Popescu, A. Jonoski, and D. Solomatine (2012). River cross-section extraction from the ASTER global DEM for flood modeling. *Environmental Modelling and Software 31*, 37–46.

Gleason, C. (2015). Hydraulic geometry of natural rivers: a review and future directions. *Progress in Physical Geography 1*, 1–24.

Hicks, F. E. (1996). Hydraulic flood routing with minimal channel data: Peace River, Canada. *Canadian Journal of Civil Engineering 23*, 524–535.

Hodges, B. (2013). Challenges in Continental River Dynamics. *Environmental Modelling and Software 50*, 16–20.

Honnorat, M., X. Lai, J. Monnier, and F. L. Dimet (2006). Variational Data Assimilation for 2D Fluvial Hydraulic Simulations. *Computational Methods in Water Resources 16*, 1–16.

Horritt, M. and P. Bates (2002). Evaluation of 1D and 2D numerical models for predicting river flood inundation. *Journal of Hydrology 268*, 87–99.

Koren, V., S. Reed, M. Smith, Z. Zhang, and D. Seo (2004). Hydrology laboratory research modeling system (HL-RMS) of the US national weather service. *Journal of Hydrology 291*, 297–318.

Leopold, L. and T. Maddock (1953). The hydraulic geometry of stream channels and some physiographic implications. *Geological Survey professional paper 252*, 1–56.

Leopold, L. and J. Miller (1956). Ephemeral ststream: hydraulic factors, and their relation to the drainage net. Technical report, USGS Professional Papers 282-A.

Liu, F. (2012). SPRINT user's manual. Technical report, IBM.

Maidment, D. R. (1993). *Handbook of Hydrology*. McGraw Hill.

Mason, D., M. Horritt, N. Hunter, and P. Bates (2007). Use of fused airborne scanning laser altimetry and digital map data for urban flood modeling. *Hydrological Processes 21*, 1436–1447.

Mejia, A. and S. Reed (2011). Evalstream the effects of paraparameter cross section shapes and simplified routing with a coupled distributed hydrologic and hydraulic model. *Journal of Hydrology 409*, 512–524.

Merwade, V., A. Cook, and J. Coonrod (2008). GIS techniques for creating river terrain models for hydrodynamic modeling and flood inundation mapping. *Environmental Modelling and Software 23*, 1300–1311.

Miller, J. (1958). High mountain sstream: effect of geology on channel characteristics and bed material. Technical report, New Mexico Bureau of Mines and Mineral Resources Memoir no. 4.

Moreda, F., A. Gutierrez, S. Reed, and C. Aschwanden (2009). Transitioning NWS operational hydraulics model from FLDWAV to HEC-RAS. In *ASCE Conference Proceeding*.

Niu, G., Z. Yang, K. Mitchell, F. Chen, M. Ek, M. Barlage, A. Kumar, K. Manning, D. Niyogi, E. Rosero, M. Tewari, and Y. Xia (2011). The community Noah land surface model with multiparameterization options (Noah-MP): 1. Model description and evaluation with local-scale measurements. *Journal of Geophysical Research 116*, 1–19.

Orlandini, S. and R. Rosso (1998). Parameterization of stream channel geometry in the distributed modeling of catchment dynamics. *Water Resources Research 34*, 1971–1985.

Paiva, R., W. Collischonn, and C. Tucci (2011). Large scale hydrologic and hydrodynamic modeling using limited data and a gis based approach. *Journal of Hydrology 406*, 170–181.

Park, C. (1977). World-wide variations in hydraulic geometry exponents of stream channels: analysis and some observations. *Journal of Hydrology 33*, 133–146.

Parker, G. (1979). Hydraulic Geometry of active gravel rivers. *Journal of Hydraulic Division 105*, 1185–1201.

Phillips, J. and J. Harlin (1984). Spatial dependency of hydraulic geometry exponents in a subalpine stream. *Journal of Hydrology 71*, 277–283.

Podhoranyi, M. and D. Fedorcak (2015). Inaccuracy introduced by LiDAR-generated cross sections and its impact on 1D hydrodynamic simulations. *Environmental Earth Sciences 73*, 1–11.

Pramanik, N., R. Panda, and D. Sen (2010). One dimensional hydrodynamic modeling of river flow using DEM extracted river cross-sections. *Water Resources Management 24*, 835–852.

Rhoads, B. (1991). A continuosly varying parameter model of downstream hydraulic geometry. *Water Resources and Research 27*, 1865–1872.

Rhodes, D. (1977). B-F-M diagram graphical representation and interpretation of at-a-station hydraulic geometry. *American Journal of Science 277*, 73–96.

Rhodes, D. (1987). The B-F-M diagram for downstream hydraulic geometry. *Geografiska Annaler Series a Physical Geography 69*, 147–161.

Richards, K. (1973). Hydraulic geometry and channel roughness: nonlinear system. *American Journal of Science 273*, 877–896.

Richards, K. (1976). Complex width-discharge relations in natural river section. *Geological Society of America 87*, 199–206.

Richards, K. (1982). Rivers, form and process in alluvial channels. Technical report, Methuen, London.

Roux, H. and D. Dartus (2004). Data AAssimilation Applied to Hydraulic Parameter Identification. *British Hydrological Society International Conference 1*, 1–18.

Roux, H. and D. Dartus (2008). Sensitivity analysis and predictive uncertainty using inundation observations for parameter estimation in open-channel inverse problem. *Journal of Hydraulic Engineering 134*, 541–549.

Sanyal, J., P. Carbonneau, and A. Densmore (2013). Hydraulic routing of extreme floods in a large ungauged river and the estimation of associated uncertainties: a case of study of the Damodar River, India. *Natural Hazards 66*, 1153–1177.

Schwanghart, W. and N. Kuhn (2010). TopoToolbox: a set of Matlab functions for topographic analysis. *Environmental Modelling and Software 25*, 770–781.

Singh, V., T. Chih, and Z. Deng (2003). Dogeometry hydraulic geometry relations: 1. Theoretical development. *Water Resources Research 39*, 1337–1352.

Snell, J. and M. Sivapalan (1995). On the application of the meta-channel concept: Construction of the meta-channel hydraulic geometry for a natural catchment. *Hydrological Processes 9*, 485–505.

Stall, J. and Y. Fok (1968). Hydraulic geometry of Illinois sstream. In *University of Illinios Water Resources Center Research Report no. 15*.

Stewardson, M. (2005). Hydraulic geometry of stream reaches. *Journal of Hydrology 36*, 97–111.

Tesfa, T., D. Tarboton, D. Watson, D. Schreuders, K. Baker, and M. Wallace (2011). Extraction of hyhydrologic proximity measures from DEMs using parallel processing. *Environmental Modelling and Software 26*, 1696–1709.

Trigg, M., M. Wilson, M. Bates, M. Horritt, D. Alsdorf, B. Forsberg, and M. Vega (2009). Amazon flood wave hydraulics. *Journal of Hydrology 374*, 92–105.

Tsubaki, R. and Y. Kawahara (2013). The uncertainty of local flow parameters during inundation flow over complex topographies with elevation errors. *Journal Hydrology 486*, 71–87.

Turowski, J., N. Hovius, and A. Wilson (2008). Hydraulic geometry, river sediment and the definition of bedrock channels. *Geomorphology 99*, 26–38.

Valiani, A. and V. Caleffi (2009). Analytical findings for power law cross-sections: uniform flow depth. *Advances in Water Resources 32*, 1404–1412.

Western, A. W. and B. Finlayson (1997). A method for characterising longitudinal irregularity in river channels. *Journal of Geomorphology 21*, 39–51.

Wigmosta, M., L. Vail, and D. Lettenmaier (1994). A Distributed Hydrology-Vegetation Model for complex terrain. *Water Resources Research 30*, 1665–1679.